

Chapter 5

Tangential Contact

Markus Heß and Valentin L. Popov

5.1 Introduction

The fundamental property that allows the reduction of three-dimensional contacts to one-dimensional ones is the proportionality of the incremental stiffness to the diameter of the contact area. This property is exhibited by both normal and tangential contacts. The idea behind dimensionality reduction can, therefore, be directly transferred to tangential contacts.

The tangential stiffness of a round contact with the diameter D between two elastic half-spaces is given by the equation [1]

$$k_x = DG^*, \quad (5.1)$$

where G^* is defined as

$$\frac{1}{G^*} = \frac{(2 - \nu_1)}{4G_1} + \frac{(2 - \nu_2)}{4G_2}. \quad (5.2)$$

G_1 and G_2 denote the shear moduli of the contacting bodies. Thereby, it should be noted that it is assumed that materials are “elastically similar”:

$$\frac{1 - 2\nu_1}{G_1} = \frac{1 - 2\nu_2}{G_2}, \quad (5.3)$$

which allows the tangential contact problem to be decoupled from the normal contact problem [2]. This condition is identically met for the important case of a contact between a rigid body and an incompressible elastomer (both sides of Eq. (5.3) are zero in this case).

Now, we consider a linearly elastic foundation consisting of springs with the stiffness

$$\Delta k_x = G^* \Delta x, \quad (5.4)$$

where Δx is the distance between the springs. The stiffness (5.1) is trivially reproduced with this foundation. In this chapter, we will show that the one-dimensional elastic foundation with the normal stiffness defined in Chap. 3 and the tangential stiffness (5.4) can also be used to *exactly* map tangential contacts with Coulomb friction for *arbitrarily axially-symmetric* profiles. We begin our considerations with the contact between parabolic bodies.

5.2 Tangential Contact with Friction for Parabolic Bodies

We consider a rigid three-dimensional parabolic body with the radius of curvature R that is pressed into an elastic half-space with the normal force F_N and subsequently loaded in the horizontal direction with the force F_x . We assume that the frictional forces acting in the contact can be simply described using Coulomb's law of friction with a constant coefficient of friction μ . From the theory of three-dimensional contact problems, it is known that even the application of an arbitrarily small force results in the formation of a slip domain at the boundary of the contact area, while the inner domain initially sticks [1]. With increasing tangential force, the stick domain shrinks until slip is initiated in the entire contact area. In this section, we investigate the one-dimensional mapping of the aforementioned three-dimensional contact problem (Fig. 5.1).

As before, let the indentation depth of the rigid body into the linearly elastic foundation be denoted by d . The vertical displacement of a spring at a distance x from the middle point of the contact is

$$u_z(x) = d - \frac{x^2}{2R_1}. \quad (5.5)$$

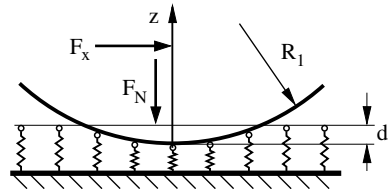
The radius R_1 must be set to $R_1 = R/2$ according to the rules of the reduction method. The elastic force of a single spring at the point x is

$$f_N(x) = E^* u_z(x) \Delta x = \left(d - \frac{x^2}{2R_1} \right) E^* \Delta x. \quad (5.6)$$

The contact radius is obtained from the condition $u_z(a) = 0$:

$$a = \sqrt{2R_1 d} = \sqrt{Rd}. \quad (5.7)$$

Fig. 5.1 One-dimensional mapping of contact loaded both normally and tangentially



Until now, we have only used the results known from Chap. 3. Now, we denote the horizontal displacement of the parabolic indenter with respect to the foundation with u_x . Then, the horizontal component of the force acting on a sticking spring is

$$f_x(x) = \Delta k_x u_x = G^* \Delta x \cdot u_x. \quad (5.8)$$

We determine the boundary of the sticking domain $x = \pm c$ from the condition that the tangential force achieves its maximum value:

$$f_x(c) = \mu f_N(c) \quad (5.9)$$

or

$$G^* \Delta x \cdot u_x = \mu \left(d - \frac{c^2}{2R_1} \right) E^* \Delta x. \quad (5.10)$$

From this, it follows that

$$c^2 = 2R_1 \left(d - \frac{G^* u_x}{E^* \mu} \right). \quad (5.11)$$

Solving with respect to u_x results in

$$u_x = \mu \frac{E^*}{G^*} \left(d - \frac{c^2}{2R_1} \right) = \mu \frac{E^*}{G^*} \left(d - \frac{c^2}{R} \right). \quad (5.12)$$

This result agrees with the result for the three-dimensional contact problem [1].

The slip condition outside of the sticking domain means that every point here fulfills Coulomb's law of friction:

$$f_x(x) = \mu f_N(x) \quad \text{for} \quad c < |x| < a. \quad (5.13)$$

Now, we calculate the normal and tangential forces acting in the entire contact area. For the normal force, we once again obtain the Hertzian result:

$$F_N = \int_{-a}^a \left(d - \frac{x^2}{2R_1} \right) E^* dx = \frac{4}{3} E^* (2R_1)^{1/2} d^{3/2} = \frac{2E^* a^3}{3R_1}. \quad (5.14)$$

The tangential force is calculated as

$$F_x = 2 \int_0^c G^* u_x dx + 2 \int_c^a \mu \left(d - \frac{x^2}{2R_1} \right) E^* dx = \frac{2E^* a^3 \mu}{3R_1} \left(1 - \left(\frac{c}{a} \right)^3 \right) = \mu F_N \left(1 - \left(\frac{c}{a} \right)^3 \right). \quad (5.15)$$

From this, the relationship between the loading and the radius of the contact area can be determined:

$$\frac{c}{a} = \left(1 - \frac{F_x}{\mu F_N} \right)^{1/3}. \quad (5.16)$$

This result also agrees exactly with that of the three-dimensional problem [1].

We obtain the displacement above which the entire contact area exhibits slip by inserting $c = 0$ into Eq. (5.12):

$$u_{x,\max} = u_x = \mu \frac{E^*}{G^*} d, \quad (5.17)$$

which, of course, also agrees exactly with that of the three-dimensional case.

5.3 Tangential Contact with Friction for Arbitrary Axially-Symmetric Bodies

In the last section, it was proven that the tangential contact with partial slip for two parabolic bodies can be exactly mapped using the method of dimensionality reduction. The generalization to tangential contacts of arbitrarily formed, axially-symmetric bodies is the topic of this chapter; the complete proofs including all assumptions can be found in Chap. 18.

In order to solve the classical three-dimensional contact problem, Cattaneo [3] and Mindlin [4] initially calculated the tangential displacement in the direction of the applied tangential force, which results from the state of full slip. Subsequently, they superimposed the corresponding tangential stress distribution with a second one of the same form, but with the opposite direction. In this way, constant tangential displacements were obtained for an inner circular area and the tangential stresses in the outer domain that are proportional to the normal stresses, which are the boundary conditions for the tangential contact with *partial* slip. Although the way was paved to solve tangential contact problems with the method of Cattaneo and Mindlin, its application to other geometries appeared exceedingly difficult, because they required explicit knowledge/calculation of the tangential displacements. Not until 50 years later did Truman et al. [5], using this method, successfully derive the solution to the tangential contact problem between a conical indenter and an elastic half-space. In the same year, Jäger [6] arrived at the conclusion that within the framework of Cattaneo-Mindlin theory, every axially-symmetric tangential contact problem can be completely described by the normal contact problem so that an explicit calculation of the tangential displacement is unnecessary. Thereby, we remember that elastically similar materials (5.3) are assumed everywhere in this chapter, which allows the contact problem to be decoupled. Furthermore, it is assumed that the frictional stresses point in the direction of the applied tangential force, which strictly speaking, violates a part of Coulomb's law of friction. Due to the addition of a slippage component perpendicular to the applied force, the tangential stresses and slip are not opposite each other at every point in the slip domain. In [7, 8], as well as Chap. 18, it is explained why we can neglect this deviation.

Due to the principle of superposition from Jäger [6, 9], the tangential stresses are equivalent to the difference between the actual normal stress and those that correspond to a smaller contact radius (the stick radius c) multiplied with the coefficient of friction. The same is true for the tangential force F_x and the relative tangential displacement u_x :

$$\tau_{zx}(r) = \mu [\sigma_{zz}(a, r) - \sigma_{zz}(c, r)] \quad (5.18)$$

$$F_x = \mu [F_N(a) - F_N(c)] \quad (5.19)$$

$$u_x = \mu \frac{E^*}{G^*} [d(a) - d(c)]. \quad (5.20)$$

It is proven in Chap. 18 that based on the Eqs. (5.18)–(5.20), these relationships can be obtained from the method of dimensionality reduction. Thus, the method already introduced within the framework of the tangential contact for a parabolic body is generally valid. It consists primarily of two central ansätze:

1. In the one-dimensional equivalent model, the tangential spring forces at the boundary of the stick domain must assume the maximum possible value for the static frictional force

$$f_x(c) = \mu f_N(c) \quad \Leftrightarrow \quad q_x(c) = \mu q(c). \quad (5.21)$$

For a given tangential displacement u_x , the radius of the stick domain c can be obtained.

2. The tangential force is given analogously to the normal force from the sum of the tangential spring forces and, therewith, the tangential distributed load

$$F_x = \int_{-a}^a q_x(x) dx = 2c G^* u_x + 2\mu \int_c^a q(x) dx. \quad (5.22)$$

On the right side, the piecewise-defined function

$$q_x(x) = \begin{cases} G^* u_x & \text{for } |x| \leq c \\ \mu q(x) & \text{for } c < |x| \leq a \\ 0 & \text{for } |x| > a \end{cases} \quad (5.23)$$

has already been inserted.

Also, based on the superposition from Jäger, the three-dimensional tangential contact with partial slip can be replaced by two three-dimensional normal contacts. This technique has already been used in various numerical simulations. It is directly evident that such a superposition also retains its validity for the equivalent one-dimensional normal contact. Nevertheless, it is preferred, and requires less effort, to directly map the three-dimensional partial slip problem to a

one-dimensional partial slip problem, rather than mapping two three-dimensional normal contacts and superimposing them.

Now, we consider an axially-symmetric indenter which has a profile with a form given by a power function with a positive real exponent

$$\tilde{z}(r) = f(r) = C_n r^n \quad (5.24)$$

and is initially pressed into an elastic half-space with the normal force F_N and subsequently, maintaining the normal force, loaded with the tangential force F_x . We are now looking for the radius of the stick domain c and the relative tangential displacement u_x of both bodies. For the normal contact, one can take the solutions from Problem 2 in Chap. 3:

$$d(a) = C_n \kappa_n a^n \quad (5.25)$$

$$F_N(a) = \frac{2n}{n+1} E^* \kappa_n C_n a^{n+1}. \quad (5.26)$$

Let us remember that the relationships above arise from the indentation of the (rigid) profile

$$g(x) = \kappa_n C_n |x|^n, \quad (5.27)$$

which is vertically scaled by the factor κ_n , into a one-dimensional linearly elastic foundation.

The extension to the tangential contact requires that the spring elements be independent from one another in the tangential direction and possess the stiffness $\Delta k_x = G^* \Delta x$. As in the three-dimensional contact problem, Coulomb's law of friction is also locally valid in the one-dimensional model. By the addition of a tangential force, the tangential springs in the area near the edge of the contact area ($c < |x| \leq a$) slide because the vertical spring forces, and therefore, the maximum frictional forces, are locally too small to satisfy the condition $f_x(x) < \mu f_N(x)$. In this domain, the spring forces (normal and tangential) at every point are directly proportional to one another: $f_x(x) = \mu f_N(x)$. Within this radius ($|x| \leq c$), all of the tangential spring elements stick and, therefore, experience the same tangential displacement u_x . In summary, the distribution of the tangential spring forces can be expressed by means of the piecewise defined distributed load

$$q_x(x) = \begin{cases} G^* u_x & \text{for } |x| \leq c \\ \mu E^* \kappa_n C_n (a^n - |x|^n) & \text{for } c < |x| \leq a \\ 0 & \text{for } |x| > a \end{cases} \quad (5.28)$$

We determine the tangential displacement u_x as a function of the radius of the stick domain c from the condition (5.21)

$$q_x(c) = \mu q(c) \quad \Rightarrow \quad u_x(c) = \mu \frac{E^*}{G^*} \kappa_n C_n (a^n - c^n). \quad (5.29)$$

The sum of all tangential spring forces must correspond to the applied tangential force, which Eq. (5.22) provides when taking (5.29) into account:

$$F_x = \frac{2n}{n+1} \mu E^* \kappa_n C_n a^{n+1} \left[1 - \left(\frac{c}{a} \right)^{n+1} \right]. \quad (5.30)$$

Solving with respect to the characteristic ratio of the contact radii and using (5.26) leads to

$$\frac{c}{a} = \left(1 - \frac{F_x}{\mu F_N} \right)^{\frac{1}{1+n}}. \quad (5.31)$$

For $n = 2$, the result of the classical contact problem from Cattaneo and Mindlin is obtained, but also the special case of a flat, cylindrical indenter can be obtained from (5.31) if we consider $n \rightarrow \infty$. As long as the tangential force F_x is smaller than the maximum static force of friction μF_N , then the *entire* contact will stick in this case. However, if this limit is reached, then complete sliding initiates. Figure 5.2 shows Eq. (5.31) graphically for the above named geometries (paraboloid and flat indenter) as well as the conical profile ($n = 1$). The gray curve is for an exponent of $n = 6$ and signifies the family of curves for increasing n .

Using the now known radius of stick, one can also determine the tangential displacement with respect to the input values. After inserting (5.31) into (5.29) and using (5.26), it follows that

$$u_x = \frac{n+1}{2n} \frac{\mu F_N}{G^* a} \left[1 - \left(1 - \frac{F_x}{\mu F_N} \right)^{\frac{n}{n+1}} \right]. \quad (5.32)$$

Naturally, Eq. (5.32) for $n = 2$ is the result for the tangential contact of a sphere [1]. For the tangential contact between a flat, cylindrical indenter and a half-space, the limit of u_x as $n \rightarrow \infty$ must once again be found, which leads to the elementary result of

$$\lim_{n \rightarrow \infty} u_x(n) = \frac{F_x}{2G^* a}. \quad (5.33)$$

Fig. 5.2 Radius of stick c as a function of applied tangential force F_x for a conical, parabolic, and flat cylindrical indenter

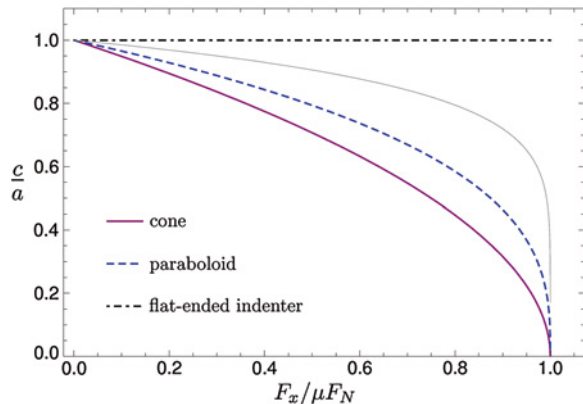
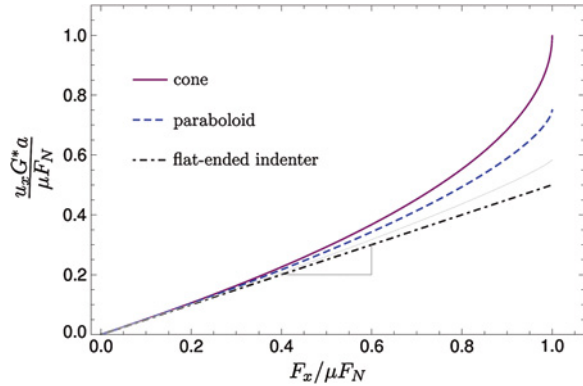


Fig. 5.3 Tangential displacement u_x plotted with respect to the tangential force F_x (normalized)



The direct proportionality between force and displacement is shown in Fig. 5.3. The slope triangle on the curve for the flat, cylindrical indenter indicates the compliance. For extremely small tangential forces, for which the slip domain is constrained to a very small ring, Eq. (5.33) is valid for all profiles, regardless of the form function exponent.

Let it once more be emphasized that the one-dimensional ansätze (5.21) and (5.22) allow for the exact mapping of tangential contacts for *arbitrary* axially-symmetric bodies. Profiles that we can describe by a *power series* as well as those that are *piecewise defined* are also included here. The latter, however, can cause difficulties, because the one-dimensional profile cannot be found simply through scaling, but must be found by integration (see Problem 3).

5.4 Mapping of Stresses in the Tangential Contact

Due to the principle of superposition from Jäger, the tangential stresses can be obtained, completely analogously to the normal stresses, from the Abel-like integral transformation of the tangential distributed load $q_x(x)$:

$$\tau_{xr}(r) = \frac{1}{\pi} \frac{1}{r} \frac{d}{dr} \int_r^a \frac{x \cdot q_x(x)}{\sqrt{x^2 - r^2}} dx = \frac{1}{\pi} \int_r^a \frac{q'_x(x)}{\sqrt{x^2 - r^2}} dx - \frac{1}{\pi} \frac{q_x(a)}{\sqrt{a^2 - r^2}}. \quad (5.34)$$

The proof for this is presented in Chap. 18. It follows from the alternate presentation of the piecewise-defined, linear force density from (5.23) as the difference between two vertical distributed loads and subsequent use of (5.18).

As an example, we want to use Eq. (5.34) on the classical tangential contact between a parabolic body and a plane. In the first step, we define the tangential

linear load for the one-dimensional model, which we already implicitly drew upon for the calculation of the tangential force in (5.15):

$$q_x(x) = \begin{cases} G^* u_x & \text{for } |x| \leq c \\ \mu E^* \left(d - \frac{x^2}{R} \right) & \text{for } c < |x| \leq a \\ 0 & \text{for } |x| > a \end{cases} \quad (5.35)$$

In order to keep the effort required to a minimum, we use the integral expression on the right side of (5.34),¹ which requires the derivative of the linear load:

$$q'_x(x) = \begin{cases} 0 & \text{for } |x| \leq c \vee |x| > a \\ -2\mu E^* \frac{x}{R} & \text{for } c < |x| \leq a \end{cases} \quad (5.36)$$

By inserting (5.36) into (5.34), we must differentiate between the two cases $0 \leq r < c$ and $c \leq r \leq a$ and, therefore, obtain

$$\tau_{zr}(r) = -\frac{2\mu E^*}{R\pi} \cdot \begin{cases} \int_c^a \frac{x}{\sqrt{x^2 - r^2}} dx & \text{for } 0 \leq r < c \\ \int_r^a \frac{x}{\sqrt{x^2 - r^2}} dx & \text{for } c \leq r \leq a \end{cases} \quad (5.37)$$

After simple integration, we obtain

$$\tau_{zr}(r) = -\frac{2\mu E^*}{R\pi} \left[\sqrt{a^2 - r^2} \cdot H\left(1 - \frac{r}{a}\right) - \sqrt{c^2 - r^2} \cdot H\left(1 - \frac{r}{c}\right) \right], \quad (5.38)$$

where $H(x)$ is the Heaviside step function. It is generally known that Eq. (5.38) corresponds to the exact distribution of the tangential stress in a three-dimensional contact [1].

5.5 Mapping of Local Slip

The micro-slip in the outer area of a tangential contact is generally described by the *local slip* $s_{x,3D}(r)$. This denotes the tangential relative displacement of the surface points in the slip domain of the contact area, which is required for the calculation of wear and other tribological processes. For the sake of clarity, the constant tangential displacement of all points within the sticking domain will be denoted in the section with

$$u_x(r) = \delta_x = \text{const. for } 0 \leq r \leq c. \quad (5.39)$$

¹ Let it be noted that in special cases of non-differentiable form functions, only the first integral expression in (5.34) may be used.

The fact that this displacement can be mapped exactly by the method of dimensional reduction has already been shown. In a similar way, the local slip in the slip domain can be reproduced as

$$s_{x,3D}(r) := u_x(r) - \delta_x \text{ for } c < r \leq a. \quad (5.40)$$

Once again, Jäger's principle of superposition is at the center of our considerations. Using this, the following equation for the slip of an axially-symmetric contact obtained from the slip in a one-dimensional model $s_{x,1D}(x)$ can be easily understood:

$$s_{x,3D}(r) = \frac{2}{\pi} \int_0^r \frac{s_{x,1D}(x)}{\sqrt{r^2 - x^2}} dx \quad \text{with} \quad s_{x,1D}(x) = u_x(x) - \delta_x. \quad (5.41)$$

Here, $u_x(x)$ is the tangential displacement of the surface of the linearly elastic foundation.

For the classical tangential contact of a parabolic body with a plane, the application of the transformation (5.41) will be explained in the following. For this, we first introduce slip in the one-dimensional model. From the tangential distributed load according to (5.35), the tangential displacements can be directly found for the equivalent system. This is because both are proportional to each other, whereby the effective shear modulus G^* is the proportionality factor:

$$u_x(x) = \begin{cases} \delta_x & \text{for } |x| \leq c \\ \mu \frac{E^*}{G^*} \underbrace{\left(d(a) - \frac{x^2}{R} \right)}_{=u_z(x)} & \text{for } c < |x| \leq a. \end{cases} \quad (5.42)$$

With this, the following is valid for the one-dimensional slip:

$$s_{x,1D}(x) := u_x(x) - \delta_x = \begin{cases} 0 & \text{for } |x| \leq c \\ \mu \frac{E^*}{G^*} \left(d(c) - \frac{x^2}{R} \right) & \text{for } c < |x| \leq a. \end{cases} \quad (5.43)$$

Insertion of (5.43) into (5.41) results initially in

$$s_{x,3D}(r) = \frac{2\mu E^*}{\pi R G^*} \int_c^r \frac{c^2 - x^2}{\sqrt{r^2 - x^2}} dx \text{ for } c < r \leq a \quad (5.44)$$

and after simple calculation, we find the three-dimensional slip from Johnson [7] in the domain of micro-slip:

$$s_{x,3D}(r) = \frac{\mu E^*}{\pi R G^*} \left[\left(2c^2 - r^2 \right) \cdot \left(\frac{\pi}{2} - \arcsin \left(\frac{c}{r} \right) \right) - c \cdot \sqrt{r^2 - c^2} \right]. \quad (5.45)$$

5.6 Problems

Problem 1 Determine the radius of stick and the relative tangential displacement with respect to the tangential force for the tangential contact between an elastic cone and an elastic half-space. Elastically similar materials are assumed. It is also assumed that the normal contact problem for which tangential loading is investigated has already been solved (see Problem 1 in Chap. 3)

Solution The equivalent one-dimensional contact problem consists of a rigid cross-section of a conical indenter scaled vertically by a factor of $\kappa_1 = \pi/2$, which is pressed into a one-dimensional linearly elastic foundation and subsequently loaded with a tangential force. All tangential spring elements whose spring forces have not yet reached the spatially-dependent maximum static force of friction $\mu f_N(x)$ undergo the respective displacement u_x . In the outer ring, the vertical spring forces, and therefore, the force of static friction, is so small that partial sliding occurs. At the stick-slip limit, the tangential spring forces must assume the maximum force of static friction

$$G^* \Delta x u_x(c) = \mu E^* \Delta x [d - g(c)], \quad (5.46)$$

which results in *constant* tangential displacement of all points in the stick domain:

$$u_x(x) = \mu \frac{\pi E^* \tan \theta}{2 G^*} (a - c) \quad \text{for } |x| \leq c. \quad (5.47)$$

In equilibrium, the tangential force F_x must be equal to the sum of the tangential spring forces:

$$\begin{aligned} F_x &= G^* \int_{-a}^a u_x(x) dx = 2G^* \int_0^c u_x(x) dx + 2\mu E^* \int_c^a u_z(x) dx \\ &= \frac{\pi}{2} \mu E^* \tan(\theta) a^2 \left[1 - \left(\frac{c}{a} \right)^2 \right]. \end{aligned} \quad (5.48)$$

By taking the results of the normal contact problems into account (see Problem 1 from Chap. 3), Eqs. (5.47) and (5.48) can be brought into the following form:

$$\frac{c}{a} = \sqrt{1 - \frac{F_x}{\mu F_N}} \quad (5.49)$$

$$u_x = \frac{\mu F_N}{G^* a} \left[1 - \sqrt{1 - \frac{F_x}{\mu F_N}} \right]. \quad (5.50)$$

Of course, these equations also result from (5.31) and (5.32) for $n = 1$ and correspond exactly with the three-dimensional solution from Truman et al. [5].

Problem 2 Calculate the tangential stress distribution within the contact area for the tangential contact handled in Problem 1 with the help of the Abel transformation in Eq. (5.34).

Solution The calculation of the three-dimensional tangential stress from the one-dimensional model requires setting up the equation for and subsequently differentiating the tangential linear load. The linear load was already implicitly used to find the tangential force in Eq. (5.48). Its derivative is

$$q'_x(x) = \begin{cases} 0 & \text{for } |x| \leq c \text{ and } |x| > a \\ -\mu E^* \frac{\pi}{2} \tan \theta \cdot \text{sign}(x) & \text{for } c < |x| \leq a \end{cases}. \quad (5.51)$$

Inserting (5.51) into Eq. (5.34) initially provides

$$\tau_{zr}(r) = -\frac{1}{2}\mu E^* \tan \theta \cdot \begin{cases} \int_c^a \frac{1}{\sqrt{x^2 - r^2}} dx & \text{for } 0 \leq r < c \\ \int_r^a \frac{1}{\sqrt{x^2 - r^2}} dx & \text{for } c \leq r \leq a \end{cases}, \quad (5.52)$$

and after integration and simple rearrangement,

$$\tau_{zr}(r) = -\frac{1}{2}\mu E^* \tan \theta \left[\text{arcosh}\left(\frac{a}{r}\right) \cdot H\left(1 - \frac{r}{a}\right) - \text{arcosh}\left(\frac{c}{r}\right) \cdot H\left(1 - \frac{r}{c}\right) \right]. \quad (5.53)$$

The tangential stress distribution, normalized by the mean value in the case of complete sliding, is plotted in Fig. 5.4 for sizes of the stick domain. The finite value at the point $r = 0$ is

$$\lim_{r \rightarrow 0} \frac{-\tau_{zr}(r)}{\mu p_m} = \lim_{r \rightarrow 0} \left[\text{arcosh}\left(\frac{a}{r}\right) - \text{arcosh}\left(\frac{c}{r}\right) \right] = \lim_{r \rightarrow 0} \ln \left(\frac{a + \sqrt{a^2 - r^2}}{c + \sqrt{c^2 - r^2}} \right) = \ln \left(\frac{a}{c} \right). \quad (5.54)$$

Fig. 5.4 Normalized tangential stress distribution with respect to the size of the stick domain $c/a = 0.1, 0.2, \dots, 1$

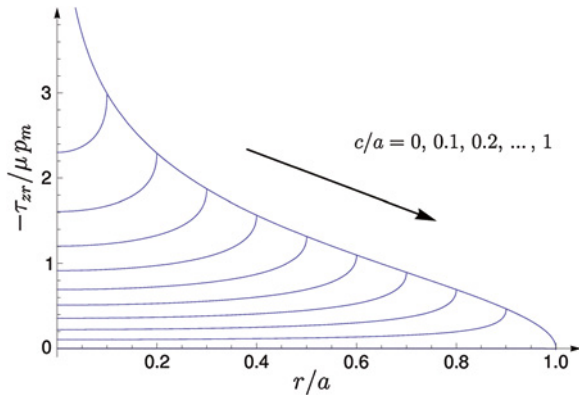
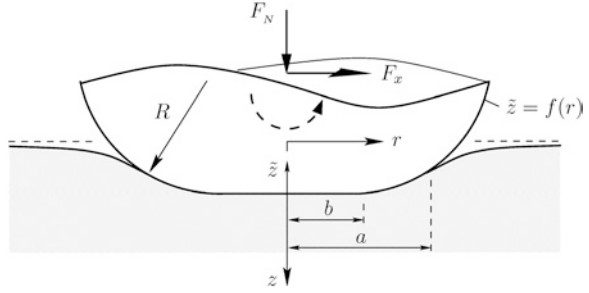


Fig. 5.5 Tangential contact of a flat indenter with rounded edges (radius R)



Problem 3 A flat, cylindrical indenter with rounded edges is initially pressed into an elastic half-space with the normal force F_N and subsequently loaded with a (presently unknown) tangential force F_x , which results in a given relative tangential displacement u_x of the two bodies. It is assumed that the bodies are composed of elastically similar materials and that the profile of the indenter is given by the following (see Fig. 5.5):

$$f(r) = \begin{cases} 0 & \text{for } 0 \leq r < b \\ \frac{1}{2R}(r-b)^2 & \text{for } b \leq r \leq a \end{cases}. \quad (5.55)$$

Determine the indentation depth and normal force as a function of contact radius with the help of the reduction method. Furthermore, calculate the tangential displacement and tangential force as a function of the stick radius.

Solution In the first step, the one-dimensional equivalent profile must be determined. The piecewise-defined function according to (5.55) requires the application of the generalized formula (3.27)

$$g(x) = x \int_0^x \frac{f'(r)}{\sqrt{x^2 - r^2}} dr = \begin{cases} 0 & \text{for } 0 \leq x < b \\ \frac{x}{R} \int_b^x \frac{r-b}{\sqrt{x^2 - r^2}} dr & \text{for } b \leq x \leq a \end{cases}. \quad (5.56)$$

Calculating the integral in Eq. (5.56) requires nothing more than elementary mathematics:

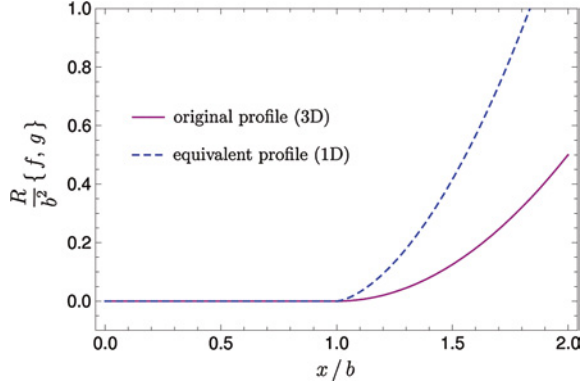
$$\int_b^x \frac{r-b}{\sqrt{x^2 - r^2}} dr = \sqrt{x^2 - b^2} - b \arccos\left(\frac{b}{x}\right). \quad (5.57)$$

Nevertheless, we must remember that (5.56) has to be extended axis-symmetrically to the domain of $-a \leq x \leq 0$. Then, we obtain

$$g(x) = \begin{cases} 0 & \text{for } |x| < b \\ \frac{|x|}{R} \sqrt{x^2 - b^2} - \frac{b|x|}{R} \arccos\left(\frac{b}{|x|}\right) & \text{for } b \leq |x| \leq a \end{cases}. \quad (5.58)$$

The normalized original and equivalent profiles are shown in Fig. 5.6.

Fig. 5.6 Flat indenter with rounded edges: Comparison between the three-dimensional and one-dimensional profiles



The indentation depth as a function of the contact radius is found from the one-dimensional profile using

$$d = g(a) = \frac{a}{R} \sqrt{a^2 - b^2} - \frac{ba}{R} \arccos \left(\frac{b}{a} \right), \quad (5.59)$$

while the dependence of the normal force on the contact radius is found from the sum of all spring forces in the contact for the one-dimensional model:

$$\begin{aligned} F_N &= 2E^* \int_0^a [d - g(x)] dx \\ &= 2E^* \int_0^b d dx + 2E^* \int_b^a \left[d - \left(\frac{x}{R} \sqrt{x^2 - b^2} - \frac{bx}{R} \arccos \left(\frac{b}{x} \right) \right) \right] dx. \end{aligned} \quad (5.60)$$

Integration, taking (5.59) into account, and rearranging results in

$$F_N = \frac{4}{3} E^* \frac{a^3}{R} \left[\left(1 - \frac{1}{4} \left(\frac{b}{a} \right)^2 \right) \sqrt{1 - \left(\frac{b}{a} \right)^2} - \frac{3}{4} \frac{b}{a} \arccos \left(\frac{b}{a} \right) \right]. \quad (5.61)$$

The limiting case of $b = 0$ is a parabolic profile. As expected, the Eqs. (5.59) and (5.61) reproduce in this limit the Hertzian relations.

The boundary between slip and stick can be found using Eq. (5.21), in other words, requiring that the tangential spring force reaches the maximum possible force of static friction at the point $x = c$. With the help of (5.58) and (5.59), one of the relationships is found:

$$u_x = \mu \frac{E^*}{G^*} \frac{a}{R} \left[\sqrt{a^2 - b^2} - b \arccos \left(\frac{b}{a} \right) - \frac{c}{a} \left(\sqrt{c^2 - b^2} - b \arccos \left(\frac{b}{c} \right) \right) \right]. \quad (5.62)$$

Now, it is only left to find the dependence between the tangential force and the stick radius. For this, we look at a distributed load in the one-dimensional model

$$q_x(x) = \begin{cases} G^* u_x & \text{for } |x| \leq c \\ \mu E^* \left[d - \frac{|x|}{R} \left(\sqrt{x^2 - b^2} - b \arccos \left(\frac{b}{|x|} \right) \right) \right] & \text{for } c < |x| \leq a \\ 0 & \text{for } |x| > a \end{cases} \quad (5.63)$$

and integrate this over the contact width in the reduced model:

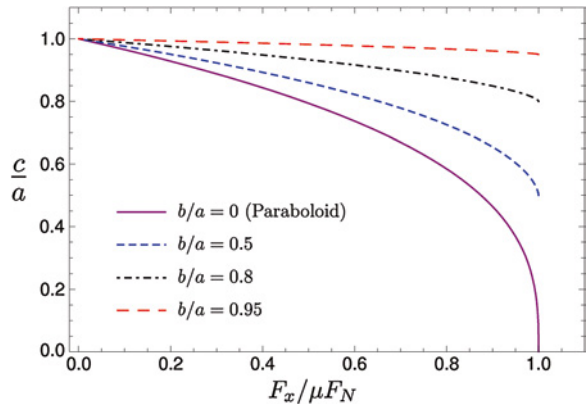
$$F_x = \int_{-a}^a q_x(x) dx = 2cG^* u_x + 2\mu E^* \int_c^a \left[d - \frac{x}{R} \left(\sqrt{x^2 - b^2} - b \arccos \left(\frac{b}{x} \right) \right) \right] dx. \quad (5.64)$$

The integral on the right-hand side already appeared in the calculation of the normal force in (5.60). After calculating the antiderivative and taking the lower limit of integration into account, we obtain

$$F_x = \mu \frac{E^*}{3R} \left[\left(4a^2 - b^2 \right) \sqrt{a^2 - b^2} - 3a^2 b \arccos \left(\frac{b}{a} \right) \right] - \mu \frac{E^*}{3R} \left[\left(4c^2 - b^2 \right) \sqrt{c^2 - b^2} - 3c^2 b \arccos \left(\frac{b}{c} \right) \right]. \quad (5.65)$$

We can be directly convinced of the correctness of Eq. (5.65) if we consider the principle of superposition by Jäger. According to (5.19), the tangential force is equivalent to the difference between the current normal force and one that would result in a stick radius c multiplied by the coefficient of friction. Using Eq. (5.61), this relationship can be easily verified. Figure 5.7 shows the normalized dependence of the stick radius on the tangential force for various cases. The limiting case of $b = 0$ corresponds to the classical result of Cattaneo and Mindlin. In contrast, if the contact area is only slightly larger than the flat section ($b = 0.95a$), then the curve approaches that of a flat indenter. A comparison is shown in Fig. 5.2.

Fig. 5.7 Stick radius c as a function of applied tangential force F_x for a flat indenter with rounded edges



Although it has not yet been mentioned, it was assumed in the above calculations that $b \leq c \leq a$, and therefore, partial sliding within the flat section is not possible. Figure 5.7 emphasizes the validity of this assumption. As soon as the slip domain includes the rounded edges, then the transition to complete slip takes place. For the analogous planar contact problem, a corresponding behavior was analytically proven [10] and verified by finite element calculations [11].

Problem 4 Determine the integral form for the normal and tangential stress distribution for the contact between a flat indenter with rounded edges having a radius of curvature of R and a half-space (see Fig. 5.5). Assume a constant distributed loading of the one-dimensional model and visualize the numeric solutions of the integral expressions.

Solution The vertical distributed load in the one-dimensional model is directly proportional to the normal displacement of the surface and according to Eq. (5.58) is

$$q(x) = \begin{cases} d & \text{for } |x| \leq b \\ E^* \left[d - \frac{|x|}{R} \left(\sqrt{x^2 - b^2} - b \arccos \left(\frac{b}{|x|} \right) \right) \right] & \text{for } b < |x| \leq a \\ 0 & \text{for } |x| > a \end{cases} \quad (5.66)$$

The derivative is required for the calculation of the normal stress distribution. Because of axial symmetry, we only have to determine this for positive x :

$$q'(x) = \begin{cases} 0 & \text{for } 0 \leq x < b \quad \vee \quad x > a \\ -\frac{E^*}{R} \left[2\sqrt{x^2 - b^2} - b \arccos \left(\frac{b}{x} \right) \right] & \text{for } b \leq x \leq a \end{cases} \quad (5.67)$$

According to Eq. (3.37) from Chap. 3, the normal stress is

$$\sigma_{zz}(r) = \begin{cases} -\frac{E^*}{\pi R} \int_b^a \frac{2\sqrt{x^2 - b^2} - b \arccos(b/x)}{\sqrt{x^2 - r^2}} dx & \text{for } 0 \leq r < b \\ -\frac{E^*}{\pi R} \int_r^a \frac{2\sqrt{x^2 - b^2} - b \arccos(b/x)}{\sqrt{x^2 - r^2}} dx & \text{for } b \leq r \leq a \end{cases} \quad (5.68)$$

These integral relations are identical to those of the three-dimensional theory. They must be solved numerically. Figure 5.8 shows the distribution of the normal stress in normalized form, where $p_m := F_N/\pi a^2$ is the mean stress. Several ratios of the length of the flatness b and the contact radius a are shown. For $b = 0$, we understandably obtain the Hertzian results, while for $b \rightarrow a$, we obtain the singularity at the edges of the contact for a flat, cylindrical indenter (with sharp edges). The presence of rounded edges guarantees a finite maximum in stress, which decreases with b/a towards the center.

The calculation of the tangential stress follows completely analogously. The tangential distributed load of the linearly elastic foundation was already shown in Problem 3 so that we must now only focus on $0 \leq x \leq a$ and differentiate (5.63) with respect to x :

$$q'_x(x) = \begin{cases} 0 & \text{for } 0 \leq x < c \quad \vee \quad x > c \\ -\frac{\mu E^*}{R} \left[2\sqrt{x^2 - b^2} - b \arccos \left(\frac{b}{x} \right) \right] & \text{for } c \leq x \leq a \end{cases} \quad (5.69)$$

Fig. 5.8 Distribution of the normalized stress for the contact in Fig. 5.5; the cases shown are those from Problem 3: $b/a = 0$ (Hertzian pressure distribution) as well as $b/a = 0.5, 0.8$, and 0.95

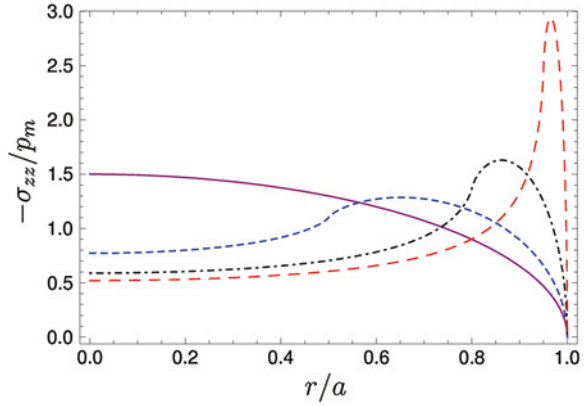
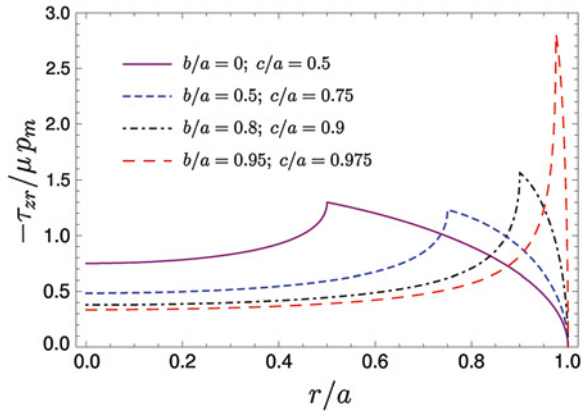


Fig. 5.9 Distribution of the tangential stress for the chosen values; the values are normalized by the average tangential stress in the case of complete sliding

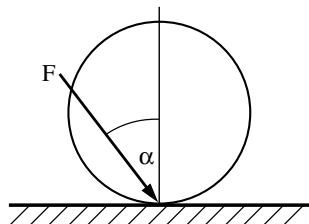


Insertion of (5.69) into (5.34) results in the distribution of the tangential stress in integral form, which corresponds to (5.68) with the exception of the integral boundaries:

$$\tau_{zr}(r) = \begin{cases} -\frac{\mu E^*}{\pi R} \int_c^a \frac{2\sqrt{x^2 - b^2} - b \arccos(b/x)}{\sqrt{x^2 - r^2}} dx & \text{for } 0 \leq r < c \\ -\frac{\mu E^*}{\pi R} \int_r^a \frac{2\sqrt{x^2 - b^2} - b \arccos(b/x)}{\sqrt{x^2 - r^2}} dx & \text{for } c \leq r \leq a \end{cases} \quad (5.70)$$

Numerically solving (5.70) leads to the normalized trend in Fig. 5.9 for the chosen values $b \leq c \leq a$. A comparison with Fig. 5.8 allows the principle of superposition from Jäger to be clearly seen; especially for $b = 0$ and the arbitrarily chosen ratio of stick to contact radius $c/a = 0.5$, the classical solution from Cattaneo and Mindlin is evident.

Fig. 5.10 Elastic sphere that is pressed by an inclined force onto a rigid half-space



The equations for the normal and tangential stresses according to (5.68) and (5.70) obtained from the distributed load in the one-dimensional model, occur identically in the three-dimensional theory [12].

Problem 5 An elastic sphere is pressed onto a rigid half-space, for which the direction of the indentation force always remains the same (Fig. 5.10). Determine the conditions under which the entire contact area sticks.

Solution In contrast to the three-dimensional case, the solution is trivial within the framework of the reduction method. Due to the fact that every sticking spring is loaded by the angle α , there is no sliding if the angle is smaller than the frictional angle [1]:

$$\tan \alpha < \mu. \quad (5.71)$$

The result is, as expected, exactly the same as that for the three-dimensional solution.

Problem 6 *Fretting wear*. Consider a rotationally symmetric profile which is brought into contact with a rigid surface and then oscillates in tangential direction with a given amplitude $u_x^{(0)}$. For small oscillation amplitudes, the wear occurs only in a circular slip zone at the border of the contact area. With increasing number of cycles, the wear profile tends to a limiting form, in which no further wear occurs. Under assumption of a constant coefficient of friction, the limiting form of the wear profile does not depend on the particular wear criterion. Using the method of dimensionality reduction, determine analytically this limiting form (for details see [13]).

Solution Assume that the friction can be described by a local formulation of the Amonton's law: The surfaces in contact are in the sticking state if tangential stress τ is smaller than normal pressure p multiplied with a constant coefficient of friction μ , and the tangential stress remains constant after the onset of sliding:

$$\begin{aligned} \tau &< \mu p, \text{ stick} \\ \tau &= \mu p, \text{ slip} \end{aligned} \quad (5.72)$$

At the circular border of the stick region with radius c , the critical condition $\tau(c) = \mu p(c)$ is fulfilled. Inside this region, the condition $\tau < \mu p$ is valid. Due to wear outside of the sticking region, the local pressure in the sticking region will increase and outside decrease further, independently of whether the experiment is

done under conditions of constant normal force or constant indentation depth d . This will lead to a progressive wear outside of the region of stick. The wear process will advance until the pressure in the sliding region becomes zero. In this limiting state, the inner parts of the contact will still remain in the sticking state, while the wear rate in the outer parts of the contact tends to zero. The final state of no wear can be considered as a sort of “shakedown” state, in which no further inelastic processes occur. The detailed kinetics of the profile depends on the wear criterion used as well as on the loading conditions (controlled force or controlled indentation). In the most cases, the Reye-Archard-Khrushchov wear criterion is used, stating that the wear volume is proportional to the dissipated energy. According to this wear criterion, the wear rate vanishes if either the relative displacement Δu_x of the bodies or tangential stress in contact is zero. In non-adhesive contacts, the latter means vanishing of the normal pressure p . The no-wear condition thus reads:

$$\text{No wear condition: } \begin{cases} \text{either } p = 0 \\ \text{or } \Delta u_x = 0 \end{cases}. \quad (5.73)$$

From these conditions, it follows that the pressure in the final state is non-zero only inside the stick area and vanishes outside.

Given a three-dimensional profile $z = f(r)$, we first determine the equivalent one-dimensional profile according to (3.27)

$$g(x) = |x| \int_0^{|x|} \frac{f'(r)}{\sqrt{x^2 - r^2}} dr. \quad (5.74)$$

The back transformation is given by the integral

$$f(r) = \frac{2}{\pi} \int_0^r \frac{g(x)}{\sqrt{r^2 - x^2}} dx. \quad (5.75)$$

The profile (5.74) is pressed to a given indentation depth d into an elastic foundation. The resulting vertical displacements of springs are given by

$$u_z(x) = d - g(x) \quad (5.76)$$

and the linear force density

$$q(x) = E^* u_z(x) = E^* (d - g(x)). \quad (5.77)$$

The contact radius a is given by the condition

$$g(a) = d. \quad (5.78)$$

The distribution of normal pressure $p = -\sigma_{zz}$ in the initial three-dimensional problem can be calculated using the integral transformation (3.37):

$$p(r) = -\frac{1}{\pi} \int_r^\infty \frac{q'(x)}{\sqrt{x^2 - r^2}} dx = \frac{E^*}{\pi} \int_r^\infty \frac{g'(x)}{\sqrt{x^2 - r^2}} dx. \quad (5.79)$$

If the profile is moved tangentially by $u_x^{(0)}$, the springs will be stressed both in the normal and tangential direction, and the radius c of the stick region will be given by the condition that the tangential force $k_x u_x^{(0)}$ is equal to the coefficient of friction μ multiplied with the normal force $k_z u_z(c)$:

$$G^* u_x^{(0)} = \mu E^* (d - g(c)). \quad (5.80)$$

Let us denote the initial three-dimensional profile as $f_0(r)$, the corresponding one-dimensional image as $g_0(x)$ and the limiting shakedown shapes as $f_\infty(r)$ and $g_\infty(x)$ correspondingly. As discussed above, the pressure outside the stick area must vanish in the limiting shakedown state: $p(r) = 0$, for $r > c$. From (5.79), it follows that

$$g'(x) = 0 \quad \text{and} \quad g(x) = \text{const} = g_0, \quad \text{for } c < x < a. \quad (5.81)$$

From the condition (5.76), it then follows that the one-dimensional profile in the shakedown state has the form

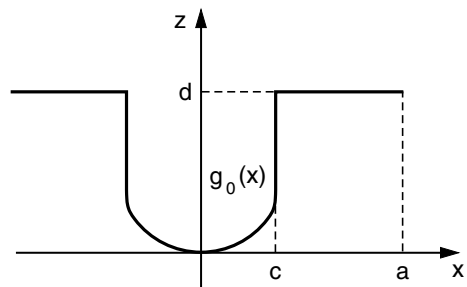
$$g_\infty(x) = \begin{cases} g_0(x), & \text{for } 0 < x < c \\ d, & \text{for } c < x < a \end{cases}. \quad (5.82)$$

This shape is schematically shown in Fig. 5.11. The three-dimensional limiting shape can now be calculated by the back transformation (5.75):

$$f_\infty(r) = \begin{cases} f_0(r) & \text{for } 0 < r < c \\ \frac{2}{\pi} \int_0^c \frac{g_0(x)}{\sqrt{r^2 - x^2}} dx + \frac{2}{\pi} d \int_c^r \frac{1}{\sqrt{r^2 - x^2}} dx, & \text{for } c < r < a \end{cases}. \quad (5.83)$$

Let us apply Eq. (5.83) to a parabolic indenter. In this case, the initial profile is $f_0(r) = r^2/(2R)$, and the corresponding one-dimensional MDR-image is $g_0(x) = x^2/R$. The radius of the stick region is given by the condition (5.80):

Fig. 5.11 One-dimensional MDR-image of the final “shakedown” profile



$$c = \sqrt{R \left(d - \frac{G^*}{E^*} \frac{u_x^{(0)}}{\mu} \right)}. \quad (5.84)$$

According to (5.83), the limiting three-dimensional profile has the form

$$f_\infty(r) = \begin{cases} \frac{r^2}{2R}, & \text{for } 0 < r < c \\ d - \frac{2}{\pi} \left(d - \frac{r^2}{2R} \right) \arcsin \frac{c}{r} - \frac{r^2}{\pi R} \left(\frac{c}{r} \right) \sqrt{1 - \left(\frac{c}{r} \right)^2}, & \text{for } c < r < a \end{cases}. \quad (5.85)$$

Normalizing all vertical coordinates by the indentation depth d and horizontal coordinates by the contact radius of the initial profile, $a_0 = \sqrt{Rd}$,

$$\begin{aligned} \tilde{f} &= f/d, & \tilde{d} &= d/d = 1 \\ \tilde{r} &= r/a_0, & \tilde{x} &= x/a_0, & \tilde{c} &= c/a_0, & \tilde{a} &= a/a_0, \end{aligned} \quad (5.86)$$

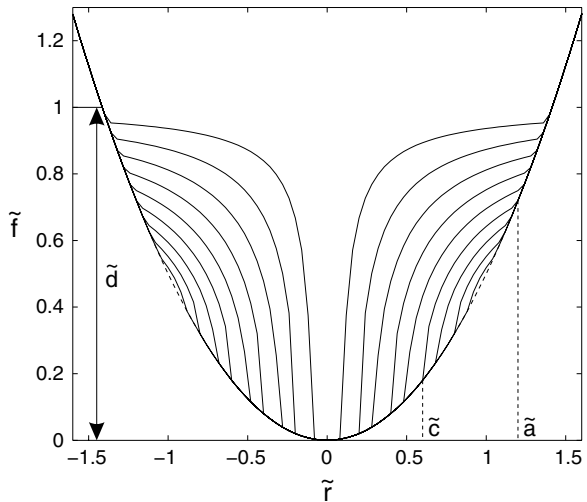
we can rewrite these equations in the dimensionless form

$$\tilde{f}_\infty(\tilde{r}) = \begin{cases} \frac{\tilde{r}^2}{2}, & \text{for } 0 < \tilde{r} < \tilde{c} \\ 1 - \frac{2}{\pi} \left(1 - \frac{\tilde{r}^2}{2} \right) \arcsin \frac{\tilde{c}}{\tilde{r}} - \frac{\tilde{r}\tilde{c}}{\pi} \sqrt{1 - \left(\frac{\tilde{c}}{\tilde{r}} \right)^2}, & \text{for } \tilde{c} < \tilde{r} < \tilde{a} \end{cases}. \quad (5.87)$$

The non-dimensional form of the limiting profile thus depends only on one parameter $0 < \tilde{c} < 1$. The contact radius, and thus the outer radius of the wear region, is given by the condition $\tilde{f}_\infty(\tilde{a}) = \tilde{f}_0(\tilde{a})$:

$$1 - \frac{2}{\pi} \left(1 - \frac{\tilde{a}^2}{2} \right) \arcsin \frac{\tilde{c}}{\tilde{a}} - \frac{\tilde{a}\tilde{c}}{\pi} \sqrt{1 - \left(\frac{\tilde{c}}{\tilde{a}} \right)^2} = \frac{\tilde{a}^2}{2}. \quad (5.88)$$

Fig. 5.12 3D profiles in the final state according to Eq. (5.87). Parameters: 9 linearly increasing \tilde{c} from 0.1 to 0.9



In the limiting case $\tilde{c} = 0$, the contact radius becomes $\tilde{a} = \sqrt{2}$.

The total force can be calculated as

$$F_N = 2 \int_0^a E^* (d - g(x)) dx = 2 \int_0^c E^* \left(d - x^2/R \right) dx = 2E^* \left(dc - \frac{c^3}{3R} \right) \quad (5.89)$$

or, under consideration of (5.84),

$$F_N = \frac{4}{3} E^* R^{1/2} \left(d - \frac{G^* u_x^{(0)}}{E^* \mu} \right)^{1/2} \left(d + \frac{G^* u_x^{(0)}}{2E^* \mu} \right). \quad (5.90)$$

Profiles (5.87) are shown in Fig. 5.12 for a representative set of parameters.

References

1. V.L. Popov, *Contact Mechanics and Friction. Physical Principles and Applications* (Springer, Berlin, 2010)
2. K.L. Johnson, *Contact Mechanics* (Cambridge University Press, Cambridge, 1985). (Chap. 7)
3. C. Cattaneo, Sul contatto di due corpi elastici: distribuzione locale degli sforzi. *Rendiconti dell'Accademia nazionale dei Lincei*. **27**, 342–348, 434–436, 474–478 (1938)
4. R.D. Mindlin, Compliance of elastic bodies in contact. *J. Appl. Mech.* **16**(3), 259–268 (1949)
5. C.E. Truman, A. Sackfield, D.A. Hills, Contact mechanics of wedge and cone indenters. *Int. J. Mech. Sci.* **37**(3), 261–275 (1995)
6. J. Jäger, Axi-symmetric bodies of equal material in contact under torsion or shift. *Arch. Appl. Mech.* **65**, 478–487 (1995)
7. K.L. Johnson, Surface interaction between elastically loaded bodies under tangential forces. *Proc. R. Soc. A* **230**, 531 (1955)
8. R.L. Munisamy, D.A. Hills, D. Nowell, Static axisymmetric hertzian contacts subject to shearing forces. *ASME J. Appl. Mech.* **61**, 278–283 (1994)
9. J. Jäger, A new principle in contact mechanics. *J. Tribol.* **120**(4), 677–684 (1998)
10. M. Ciavarella, D.A. Hills, G. Monno, The influence of rounded edges on indentation by a flat punch. *J. Mech. Eng. Sci., Proc. Inst. Mech. Eng. Part C* **212**(4), 319–328 (1998)
11. J. Jäger, New analytical solutions for a flat rounded punch compared with FEM. *Comput. Methods Contact Mech.* **5**, 307–316 (2001)
12. M. Ciavarella, Indentation by nominally flat or conical indenters with rounded corners. *Int. J. Solids Struct.* **36**, 4149–4181 (1999)
13. V.L. Popov, Analytic solution for the limiting shape of profiles due to fretting wear. *Sci. Rep.* **4**, 3749 (2014). doi:[10.1038/srep03749](https://doi.org/10.1038/srep03749)

<http://www.springer.com/978-3-642-53875-9>

Method of Dimensionality Reduction in Contact
Mechanics and Friction

Popov, V.L.; Heß, M.

2015, XVII, 265 p. 115 illus., 13 illus. in color.,

Hardcover

ISBN: 978-3-642-53875-9